Journal of Engineering Mathematics 20 (1986) 113–126

Distributions of sources and normal dipoles over a quadrilateral panel

J.N. NEWMAN

Department of Ocean Engineering, Massachusetts Institute of Technology, Cambridge, MA 02139, USA

(Received May 2, 1985 and in final form September 3, 1985)

Summary

The potential due to a distribution of sources or normal dipoles on a flat quadrilateral panel is evaluated for the cases where the density of the singularities is constant, linear, bilinear, or of arbitrary polynomial form. The results in the first two cases are consistent with those derived previously, but the present derivation is considered to be simplified. In particular, the constant dipole distribution is derived from a geometric argument which avoids direct integration; this derivation applies more generally on a curvilinear panel bounded by straight edges.

Also presented are multipole expansions for the same potentials, suitable for use when the distance to the field point is substantially larger than the panel dimensions. Algorithms are derived to evaluate the coefficients in these expansions to an arbitrary order.

1. Introduction

A wide variety of practical problems in hydro- and aerodynamics may be solved using boundary-integral methods, with the velocity potential constructed from distributions of sources and normal dipoles on each panel of the discretized boundary surface. If the strength of the singularities is assumed constant on each panel, and the boundary-integral equation is solved by collocation, a linear system of algebraic equations results with canonical matrix elements given by unit-strength distributions on each panel. These must be evaluated at appropriate nodal points on every panel. With N panels used to describe the body surface, there are $N \times N$ matrix elements for both the source and normal dipole. Typical three-dimensional solutions require on the order of 1000 panels, with $O(10^6)$ matrix elements to be evaluated. The computation of these elements is an important task in the numerical solution.

Hess and Smith [1–3] introduced this general technique, using constant-strength distributions on quadrilateral flat panels, and derived closed-form expressions from the matrix elements by evaluating analytically the surface integrals over each panel. One concept stressed in the first two references is that a surface integral over the quadrilateral panel (or more generally over a polygonal panel with an arbitrary number of sides) can be expressed as a superposition of integrals over a set of infinite parallel strips. Each strip is defined by one side of the panel, and the value of the corresponding integral depends only on the coordinates of that side. This decomposition is effective in the algorithmic sense, since the computations can be performed in sequence for each side. In a simpler and more

direct approach followed by Hess and Smith [3], the surface integral for the source distribution is reduced to a line integral around the perimeter of the panel, with the same implication that the contribution from each side can be treated independently.

In subsequent extensions linear distributions have been used on triangular panels to provide a more continuous description of the solution. The appropriate matrix elements for these distributions have been derived by Yeung [4] and Webster [5]. However the fundamental connections which exist between their results and those obtained by Hess and Smith do not appear to be appreciated.

A more unified derivation including and extending these earlier analyses is the objective of the present paper. First, it will be shown that the potential due to a normal dipole distribution with constant moment can be derived from an appropriate sum of surface integrals over infinite sectors, corresponding to each vertex of the panel and bounded by semi-infinite extensions of the adjacent sides of the panel. In this way the dipole potential may be expressed as a sum of terms depending only on the properties of each vertex, as opposed to each side. The latter feature could be deduced directly from the result of Hess and Smith, simply by regrouping of the pairs of terms in their equations. However, the derivation used here employs the Gauss-Bonnet theorem to evaluate the dipole potential directly, in terms of the included angle of each vertex projected on a plane normal to the axis between the vertex and the field point. In this manner the analysis associated with direct integration over the panel surface can be avoided. An additional feature of the present derivation is that it is valid for an arbitrary curvilinear panel surface bounded by straight segments.

In view of the equivalence between the constant dipole distribution and a vortex filament surrounding the panel, this method can also be used in lifting-surface applications to derive the velocity potential of a vortex lattice.

The corresponding result for a source distribution of constant strength on a flat panel is obtained by integration from the dipole distribution, and involves only one elementary integral. Although the approaches differ, this portion of our analysis appears algebraically similar to that presented by Hess and Smith [3].

For the linear distributions of singularities two canonical integrals are considered for the source potential, and evaluated with recourse to only one elementary integral. The corresponding results for the dipole are obtained in a similar manner. The potentials for singularities of constant strength are utilized to simplify the analysis. The same approach is used to derive a bilinear source distribution, which provides a representation of continuous singularity distributions on quadrilateral panels.

A more general recursive scheme is developed in Section 5 to evaluate source and dipole distributions of arbitrary higher-order polynomial form.

Section 6 is devoted to a far-field multipole approximation of the above results. The efficiency of such an approach is emphasized by Hess and Smith [1,2] with a point source and quadrupoles used in place of the constant-strength source distribution when the field point is sufficiently far from the panel. The corresponding strengths of these point singularities are the area and second moments, respectively, of the panel. (The dipole terms proportional to the first moments are eliminated by locating the point singularities at the centroid of the panel.) We extend this technique to include linear and higher-order distributions, and we retain additional terms in the multipole expansions proportional to the third and fourth moments of the panel area. The latter extension increases the accuracy of the far-field approximation, and extends its domain of application. Algorithms are described for computing arbitrary moments of each panel.

2. Dipole distribution of constant density

A flat quadrilateral panel will be assumed for the analysis, following the convention of Hess and Smith. It may be assumed without loss of generality that the panel is in the plane $z = 0$, with vertices at the points $x = \xi_n$, $y = \eta_n$. The vertices are numbered in clockwise order, as shown in Figure 1, and the side of length s_n is denoted by the integer of the vertex associated with the first end point of that side. The field point is at an arbitrary position P with coordinates (x, y, z).

The potential at P due to a distribution of normal dipoles with density -4π over this panel is

$$\Phi = \iint \left[\frac{\partial}{\partial \zeta}\left(\frac{1}{r}\right)\right]_{\zeta=0} \mathrm{d}\xi\, \mathrm{d}\eta = -\iint \left[\frac{\partial}{\partial z}\left(\frac{1}{r}\right)\right]_{\zeta=0} \mathrm{d}\xi\, \mathrm{d}\zeta$$

$$= z \iint \left[(x-\xi)^2 + (y-\eta)^2 + z^2\right]^{-3/2} \mathrm{d}\xi\, \mathrm{d}\eta \tag{2.1}$$

where the surface integrals are over the domain of the panel. From reciprocity, the last form of this equation can be associated with the flux through the panel due to a source of strength -4π at the point P. It follows that the value of (2.1) is equal to the solid angle of the panel, as viewed from the field point P, with the algebraic convention that the sign of the solid angle is the same as z.

First we note from elementary plane geometry that the solid angle of the panel can be related to independent properties of each vertex. For this purpose four sectors are defined with respect to the corresponding vertices, as shown in Figure 2, such that the difference between the domains of the first and second sectors, plus the corresponding difference between the third and fourth sectors, is the domain of a quadrilateral. If the value of the surface integral over each sector, with the same integrand as (2.1), is defined by I_n, it follows that

$$\Phi = I_1 - I_2 + I_3 - I_4. \tag{2.2}$$

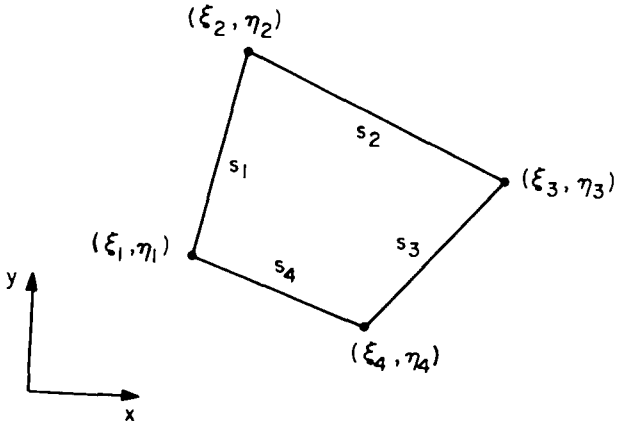

Figure 1. Definition sketch of the quadrilateral panel.

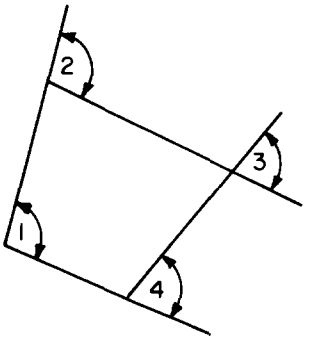

Figure 2. The four sectors for the integrals I_n.

In accordance with the interpretation following (2.1), each of the integrals in (2.2) is equal to the solid angle of the corresponding sector referred to the point P.

A more direct and useful result follows from the Gauss-Bonnet theorem in differential geometry: if the quadrilateral panel is projected onto the unit sphere, with center at the field point, the area circumscribed by its boundary contour (and hence the solid angle) is equal to the sum

$$\Phi = \beta_1 + \beta_2 + \beta_3 + \beta_4 - 2\pi. \tag{2.3}$$

Here β_n is the included angle at each vertex on the sphere. For a triangular panel, the last term in (2.3) is replaced by $-\pi$, and for a polygon with N sides by $-(N-2)\pi$.

The included angle of a vertex may be measured in the tangent plane on the sphere, or in any plane perpendicular to the vector between the field point and the vertex. It is sufficient to consider a single vertex, say $n = 1$. To simplify the following equations it will be assumed that this vertex is at the origin; subsequently the coordinates (x, y) of the field point P will be replaced by the differences $(x - \xi_n, y - \eta_n)$ to provide the more general result for a vertex at (ξ_n, η_n). The essential task is to determine the included angle between two radial lines in the plane $z = 0$, with polar angles θ_4 and θ_1, as viewed from a point P with arbitrary coordinates (x, y, z). Here θ_n is defined as the polar angle of the vector from the vertex n to the vertex $n + 1$.

Spherical coordinates may be used in a straightforward manner. If the coordinates of P are given by

$$x + \mathrm{i}y = R \sin\phi \, \mathrm{e}^{\mathrm{i}\alpha}, \tag{2.4}$$

$$z = R \cos\phi, \tag{2.5}$$

one may rotate first about the z-axis through an angle α, and then through an angle ϕ about the axis normal to $0z$ and $0P$, to obtain new Cartesian coordinates (u, v, w) where P is at $(0, 0, R)$. In this transformation the projections on the u, v-plane of the two radial lines defined above, in the x, y-plane, are the rays

$$\frac{u}{v} = \frac{\cos\phi \cos(\theta_n - \alpha)}{\sin(\theta_n - \alpha)}, \quad n = 1, 4. \tag{2.6}$$

The included angle β_1 between these rays is therefore given by the expression

$$\beta_1 = \tan^{-1}\left[\frac{\tan(\theta_1 - \alpha)}{\cos\phi}\right] - \tan^{-1}\left[\frac{\tan(\theta_4 - \alpha)}{\cos\phi}\right]. \tag{2.7}$$

An alternative form can be derived from a different pair of rotations, in terms of the spherical coordinates such that

$$x + iz = R \sin\delta\, e^{i\psi}, \tag{2.8}$$

$$y = R\cos\delta. \tag{2.9}$$

Rotating first about the y-axis through the angle ψ, and then about the axis normal to $0y$ and $0P$ through the angle δ, new Cartesian coordinates (u, v, w) follow where the coordinates of P are $(0, R, 0)$, and the projections of the rays in the x, y-plane on the w, u-plane are along the lines

$$\frac{u}{w} = \frac{\cos\theta\cos\psi\cos\delta - \sin\theta\sin\delta}{-\cos\theta\sin\psi}. \tag{2.10}$$

With this transformation, the included angle is given by

$$\begin{aligned}\beta_1 &= \tan^{-1}\left[\frac{\tan\theta_1\sin\delta - \cos\psi\cos\delta}{\sin\psi}\right] - \tan^{-1}\left[\frac{\tan\theta_4\sin\delta - \cos\psi\cos\delta}{\sin\psi}\right] \\ &= \tan^{-1}\left[\frac{\tan\theta_1(x^2+z^2) - xy}{Rz}\right] - \tan^{-1}\left[\frac{\tan\theta_4(x^2+z^2) - xy}{Rz}\right].\end{aligned} \tag{2.11}$$

Since the arctangent is not unique, the correct branch must be determined in (2.7) or (2.11). The intent is to evaluate the solid angle Φ, a quantity between -2π and 2π with the same sign as z. For a normal quadrilateral with four concave vertices the corresponding angles β_n are between 0 and π in absolute value. For $z > 0$ the denominators of (2.11) are positive, and with the arctangent defined by its principal branch, between $-\pi/2$ and $+\pi/2$, it is not difficult to show that (2.11) will have the same sign as the difference $\tan\theta_1 - \tan\theta_4$ irrespective of the coordinates (x, y, z). For a normal quadrilateral, two of these differences are positive, and two are negative. Thus for two of the four integrals it is appropriate to add π to (2.11) to determine the solid angle. Since this addition of 2π is cancelled by the last term in (2.3), (2.3) can be replaced by the sum of the four differences (2.11). Since (2.11) is an odd function of z, the restriction $z > 0$ can be removed.

For a quadrilateral with one convex vertex, only one of the four differences (2.11) is negative, but since the solid angle of the convex vertex is between π and 2π, the application of (2.11) without any correction term in (2.3) is still correct. Thus in all cases the total solid angle of the quadrilateral is the sum of the four differences (2.11) provided the computation of the arctangent is restricted to the principal branch. In the case of a triangle, one of the three vertices will have a negative value for (2.11), which again is conveniently cancelled by the appropriate factor π, and (2.11) can be summed for the three vertices of a triangle without additional corrections.

The decomposition of the panel in terms of its vertices is convenient from the standpoint of the derivation above, but for computational purposes where the source and

dipole potentials are evaluated together, it is more efficient to pair the functions in (2.7) or (2.11) which are common to each side. First the tangents in (2.11) are expressed in terms of ratios of the vertical and horizontal components of the sides,

$$\tan \theta_1 = \frac{\eta_2 - \eta_1}{\xi_2 - \xi_1} \equiv \frac{\delta\eta_1}{\delta\xi_1}, \tag{2.12}$$

$$\tan \theta_4 = \frac{\eta_1 - \eta_4}{\xi_1 - \xi_4} \equiv \frac{\delta\eta_4}{\delta\xi_4}. \tag{2.13}$$

If (2.11) is substituted in (2.3), and the eight terms in this sum are paired in accordance with each side, it follows that

$$\Phi = \sum_{n=1}^{4} \left\{ \tan^{-1} \frac{\delta\eta_n \left[(x-\xi_n)^2 + z^2 \right] - \delta\xi_n (x-\xi_n)(y-\eta_n)}{R_n z \delta\xi_n} \right.$$
$$\left. - \tan^{-1} \frac{\delta\eta_n \left[(x-\xi_{n+1})^2 + z^2 \right] - \delta\xi_n (x-\xi_{n+1})(y-n_{n+1})}{R_{n+1} z \delta\xi_n} \right\} \tag{2.14}$$

where the cyclic convention applies. The pair of arctangents in this expression can be combined by using the trigonometric addition formulae in the form

$$\tan^{-1}(s_1/c_1) - \tan^{-1}(s_2/c_2) = \tan^{-1}(s_3/c_3) \tag{2.15}$$

where s_n and c_n are the respective factors in the numerator and denominator of each term in (2.14), for $n = 1, 2$, and s_3 and c_3 are given by the addition formulae for the sine and cosine:

$$s_3 = s_1 c_2 - s_2 c_1, \tag{2.16}$$

$$c_3 = c_1 c_2 + s_1 s_2. \tag{2.17}$$

If this algorithm is used, the last arctangent in (2.15) may be evaluated on the assumption that it is in the interval $(-\pi, \pi)$, without considering the separate arguments of the arctangents on the left side of (2.15).

The result (2.14) is identical to that of Hess and Smith. The correct numerical interpretation of (2.7) is more difficult, and this function is not well-conditioned when the field point is directly above or below a vertex. Thus (2.14), based on (2.11), is a preferable form for computations.

While the analysis above is based on the assumption of a flat panel, situated in the plane $z = 0$, the final results (2.7) and (2.11) are valid more generally for any curvilinear panel bounded by straight edges, with the dipole potential (2.1) redefined in terms of the local normal derivative on the panel surface. In this case the contribution from each vertex must be evaluated separately, in a local coordinate system which is oriented in terms of the plane sector defined by the vertex and adjacent edges, such that the latter are in the plane $z = 0$. The nonuniqueness of the arctangents must be resolved with respect to the relationship between the panel surface and the field point P, to ensure the correct jump of the potential when P crosses the surface.

3. Source distribution of constant strength

The potential of a source distribution of constant strength -4π over a flat panel can be expressed in a form analogous to (2.1) by the surface integral

$$\Psi = \iint \frac{\mathrm{d}\xi\ \mathrm{d}\eta}{r}. \tag{3.1}$$

Comparison with (2.1) indicates that $\Phi = -\partial\Psi/\partial z$, and since both functions vanish at infinity, the source potential can be expressed by the integral

$$\Psi = \int_z^\infty \Phi\ \mathrm{d}z = -\int_z^\infty z\ \mathrm{d}\Phi - z\Phi \tag{3.2}$$

where the second form follows by partial integration. The coordinates $(x,\ y)$ are constant in these integrals, and in subsequent evaluations of the differential $\mathrm{d}\Phi$.

If (2.3) and (2.7) are substituted for the dipole potential in (3.2), eight integrals of the following form must be evaluated:

$$I = -\int_z^\infty z\ \mathrm{d}\left(\tan^{-1}\left[\frac{\tan(\theta-\alpha)}{\cos\phi}\right]\right)$$

$$= -\tan(\theta-\alpha)\int_z^\infty \frac{z\cos^2\phi}{\cos^2\phi + \tan^2(\theta-\alpha)}\,\mathrm{d}(\sec\phi). \tag{3.3}$$

(Note that ϕ is the only angle dependent on z.) Using (2.5), and evaluating the last differential in (3.3) in terms of the variable $R = (x^2+y^2+z^2)^{1/2} = (\rho^2+z^2)^{1/2}$ for fixed values of the projection ρ of R on $z=0$, (3.3) can be expressed in the form

$$I = \rho^2\ \tan(\theta-\alpha)\int_z^\infty \frac{\mathrm{d}R}{\left[1+\tan^2(\theta-\alpha)\right]R^2 - \rho^2}$$

$$= -\tfrac{1}{2}\rho\ \sin(\theta-\alpha)\ \log\left[\frac{R-\rho\ \cos(\theta-\alpha)}{R+\rho\ \cos(\theta-\alpha)}\right]. \tag{3.4}$$

The eight integrals may be combined in four pairs in accordance with each side of the panel. For the side 1, shown in Figure 3, two contributions of the form (3.4) with opposite signs are associated with the two vertices, and the total contribution for this side is

$$-\tfrac{1}{2}\rho_1\ \sin(\theta_1-\alpha_1)\ \log\left[\frac{R_1-\rho_1\ \cos(\theta_1-\alpha_1)}{R_1+\rho_1\ \cos(\theta_1-\alpha_1)}\right]$$

$$+\tfrac{1}{2}\rho_2\ \sin(\theta_1-\alpha_2)\ \log\left[\frac{R_2-\rho_2\ \cos(\theta_1-\alpha_2)}{R_2+\rho_2\ \cos(\theta_1-\alpha_2)}\right]. \tag{3.5}$$

Here $\rho_1\ \exp(\mathrm{i}\alpha_1)$ and $\rho_2\ \exp(\mathrm{i}\alpha_2)$ are the complex vectors from the corresponding vertices

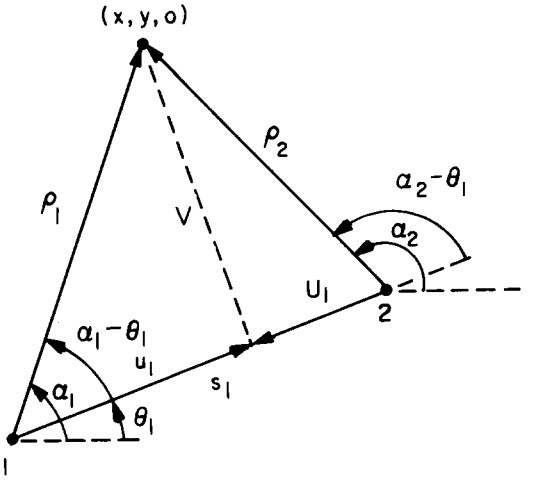

Figure 3. Sketch of the parameters in (3.5–3.7).

to the point $(x, y, 0)$, and R_1 and R_2 are the radial distances from these vertices to the field point P. The complex vector of the side, of length s_1, can be defined by

$$s_1 \, e^{i\theta_1} = \rho_1 \, e^{i\alpha_1} - \rho_2 \, e^{i\alpha_2}. \tag{3.6}$$

Rotating the polar coordinates to coincide with this side, it follows that

$$\begin{aligned} s_1 &= \rho_1 \, e^{i(\alpha_1 - \theta_1)} - \rho_2 \, e^{i(\alpha_2 - \theta_1)} \\ &\equiv (u_1 - iv_1) - (U_1 - iV_1). \end{aligned} \tag{3.7}$$

Here $(u_1, -v_1)$ and $(U_1, -V_1)$ denote the real and imaginary parts of the two vectors, in the rotated coordinate system. (This notation is necessary in order to generalize (3.7) to the n'th side without recourse to double subscripts.)

Since the sum on the right side of (3.7) must be real, $V_1 = v_1$, and the two terms in (3.5) can be combined in the form

$$\tfrac{1}{2} v_1 \log \frac{(R_2 - U_1)(R_1 + u_1)}{(R_2 + U_1)(R_1 - u_1)} \equiv v_1 Q_1 \tag{3.8}$$

where

$$\begin{aligned} Q_1 &= \frac{1}{2} \log \frac{(R_2 - U_1)(R_1 + u_1)}{(R_2 + U_1)(R_1 - u_1)} \\ &= \log \frac{R_1 + u_1}{R_2 + U_1} = \log \frac{R_2 - U_1}{R_1 - u_1} = \log \frac{R_1 + R_2 + s_1}{R_1 + R_2 - s_1}. \end{aligned} \tag{3.9}$$

The alternative forms shown in (3.9) follow from the identities $R_1^2 - u_1^2 = R_2^2 - U_1^2$ and $s_1 = u_1 - U_1$. Hess and Smith [3] recommend the last form of (3.9) for computations since

the arguments of the other logarithms are indeterminate along the extensions of the side. Note that (3.9) is logarithmically infinite when the field point approaches the side, but the factor v in (3.8) vanishes in the same limit. Thus the source potential is finite on the sides of the panel, but its gradient is unbounded.

With the factor v_n expressed in terms of the Cartesian coordinates, (3.8) may be summed over the four sides and substituted in (3.2) to yield the source potential in the form

$$\Psi = \sum_{n=1}^{4} v_n Q_n - z\Phi$$

$$= \sum_{n=1}^{4} [(x-\xi_n)\sin\theta_n - (y-\eta_n)\cos\theta_n] \log\frac{R_n + R_{n+1} + s_n}{R_n + R_{n+1} - s_n} - z\Phi. \tag{3.10}$$

The same result is derived by Hess and Smith ([3], eq. 4.1.13)). The three velocity components can be derived by differentiation of (3.10) with respect to the corresponding Cartesian coordinates, and it is not difficult to confirm that $\partial\Psi/\partial z = -\Phi$.

4. Linear and bilinear distributions

In order to extend the preceding analysis to include a linear distribution of sources and dipoles on each panel we consider two integrals, analogous to (3.1), and defined by

$$\begin{pmatrix}\Psi_x\\ \Psi_y\end{pmatrix} = \iint \begin{pmatrix}\xi\\ \eta\end{pmatrix} \frac{d\xi\, d\eta}{r}. \tag{4.1}$$

The first integral can be reduced in the following manner:

$$\Psi_x = \iint (\xi - x)\frac{d\xi\, d\eta}{r} + x\Psi$$

$$= \iint \frac{\partial r}{\partial \xi} d\xi\, d\eta + x\Psi = \oint r\, d\eta + x\Psi \tag{4.2}$$

where Ψ is the (constant-strength) source distribution evaluated in Section 3. Similarly,

$$\Psi_y = -\oint r\, d\xi + y\Psi. \tag{4.3}$$

Since the vertices and sides are defined in a clockwise sense, opposite to the convention of the contour integrals in (4.2) and (4.3), these results can be expressed in terms of integrals over each side of the panel, in the common form

$$\begin{pmatrix}\Psi_x\\ \Psi_y\end{pmatrix} = \begin{pmatrix}x\\ y\end{pmatrix}\Psi \mp \sum_{n=1}^{4} \begin{pmatrix}\sin\theta_n\\ \cos\theta_n\end{pmatrix} \int_{s_n} r\, dl. \tag{4.4}$$

The analogous dipole distributions may be defined in a similar manner:

$$\begin{pmatrix} \Phi_x \\ \Phi_y \end{pmatrix} = z \iint \begin{pmatrix} \xi \\ \eta \end{pmatrix} \frac{d\xi\, d\eta}{r^3}$$

$$= \begin{pmatrix} x \\ y \end{pmatrix} \Phi \pm z \sum_{n=1}^{4} \begin{pmatrix} \sin \theta_n \\ \cos \theta_n \end{pmatrix} \int_{S_n} \left(\frac{1}{r} \right) dl. \tag{4.5}$$

The last integrals in (4.4–4.5) can be evaluated by defining a local coordinate s, equal to the distance along each side. It follows that

$$\int_{S_n} r^{\pm 1}\, dl = \int_0^{s_n} \left[s^2 - 2u_n s + R_n^2 \right]^{\pm 1/2} ds = \begin{pmatrix} P_n \\ Q_n \end{pmatrix} \tag{4.6}$$

where u_n and Q_n are defined by (3.7–3.9), and

$$P_n = \tfrac{1}{2} \left[u_n R_n - U_n R_{n+1} + \left(R_n^2 - u_n^2 \right) Q_n \right]. \tag{4.7}$$

With these functions substituted for the integrals in (4.5–4.6), the linear-distribution integrals are evaluated in terms of the expressions

$$\begin{pmatrix} \Psi_x \\ \Psi_y \end{pmatrix} = \begin{pmatrix} x \\ y \end{pmatrix} \Psi \mp \sum_{n=1}^{4} P_n \begin{pmatrix} \sin \theta_n \\ \cos \theta_n \end{pmatrix} \tag{4.8}$$

$$\begin{pmatrix} \Phi_x \\ \Phi_y \end{pmatrix} = \begin{pmatrix} x \\ y \end{pmatrix} \Phi \pm z \sum_{n=1}^{4} Q_n \begin{pmatrix} \sin \theta_n \\ \cos \theta_n \end{pmatrix} \tag{4.9}$$

These results may be supplemented by a corresponding bilinear source or dipole distribution to permit satisfying nodal conditions at the four vertices of a quadrilateral. The bilinear source potential is defined by

$$\Psi_{xy} = \iint \xi \eta \frac{d\xi\, d\eta}{r}$$

$$= \iint (\xi - x)(\eta - y) \frac{d\xi\, d\eta}{r} + x\Psi_y + y\Psi_x - xy\Psi. \tag{4.10}$$

Following a similar procedure to that carried out above, the last double integral in (4.10) may be evaluated as follows:

$$\iint (\xi - x)(\eta - y) \frac{d\xi\, d\eta}{r} = \iint (\xi - x) \frac{\partial r}{\partial \eta} d\xi\, d\eta$$

$$= \sum_{n=1}^{4} \cos \theta_n \int_0^{s_n} r(\xi_n - x + s \cos \theta_n)\, ds. \tag{4.11}$$

Using (4.6–4.7) and the relation

$$\int_0^{s_n}(s-u_n)r\,\mathrm{d}s=\tfrac{1}{3}\int_0^{s_n}\mathrm{d}(r^3)=\tfrac{1}{3}\left(R_{n+1}^3-R_n^3\right), \tag{4.12}$$

it follows that

$$\Psi_{xy}=x\Psi_y+y\Psi_x-xy\Psi+\sum_{n=1}^{4}\cos\theta_n\left[-v_nP_n\sin\theta_n+\tfrac{1}{3}\left(R_{n+1}^3-R_n^3\right)\cos\theta_n\right]. \tag{4.13}$$

The corresponding result for the bilinear normal dipole distribution is

$$\Phi_{xy}=x\Phi_y+y\Phi_x-xy\Phi+z\sum_{n=1}^{4}\cos\theta_n\left[v_nQ_n\sin\theta_n-\left(R_{n+1}-R_n\right)\cos\theta_n\right]. \tag{4.14}$$

5. Higher-order distributions

Higher-order polynomial distributions may be considered as generalizations of the preceding results. To simplify the notation we consider the integrals

$$\begin{pmatrix}\psi_{mn}\\ \phi_{mn}\end{pmatrix}=\iint(\xi-x)^m(\eta-y)^n\begin{pmatrix}r^{-1}\\ r^{-3}\end{pmatrix}\mathrm{d}\xi\,\mathrm{d}\eta \tag{5.1}$$

which can be used in conjunction with the binomial theorem to evaluate the double integrals in (4.1) and (4.5) with arbitrary positive powers of the coordinates (ξ, η). By combining the appropriate integrands, it is straightforward to verify the relations

$$\phi_{m+2,n}=(m+1)\psi_{m,n}-\iint\frac{\partial}{\partial\xi}\left[r^{-1}(\xi-x)^{m+1}(\eta-y)^n\right]\mathrm{d}\xi\,\mathrm{d}\eta, \tag{5.2}$$

$$\phi_{m,n+2}=(n+1)\psi_{m,n}-\iint\frac{\partial}{\partial\eta}\left[r^{-1}(\xi-x)^m(\eta-y)^{n+1}\right]\mathrm{d}\xi\,\mathrm{d}\eta, \tag{5.3}$$

$$(m+n+1)\psi_{mn}+z^2\phi_{mn}=\iint\left\{\frac{\partial}{\partial\xi}\left[r^{-1}(\xi-x)^{m+1}(\eta-y)^n\right]+\frac{\partial}{\partial\eta}\left[r^{-1}(\xi-x)^m(\eta-y)^{n+1}\right]\right\}\mathrm{d}\xi\,\mathrm{d}\eta. \tag{5.4}$$

The surface integrals in (5.2–5.4) can be reduced to contour integrals, and evaluated in a manner similar to the corresponding results in Sections 3 and 4. The following procedure may then be adopted to evaluate the higher-order distributions (5.1):

(1) Evaluate the elements with (m, n) equal to (0, 0), (0, 1), (1, 0), (1, 1) from the results in Sections 2–4.

(2) Evaluate the elements ϕ_{mn} with increasing values of (m, n) recursively from (5.2, 5,3), respectively.

(3) Evaluate the corresponding elements ψ_{mn} from (5.4).
(4) Repeat steps 2 and 3 as necessary to evaluate the desired elements.

The linear and bilinear dipole distributions ($m = 1$ and/or $n = 1$) may also be evaluated from this procedure, with the first terms on the right side of (5.2) and (5.3) deleted. Similarly, all of the source distributions including the constant, linear and bilinear cases may be evaluated from the corresponding dipole results using (5.4). However, the analysis required is somewhat more complicated than the derivations of the same integrals carried out in Sections 3 and 4.

6. Multipole expansions

The exact expressions described in the preceding sections are straightforward to compute, but for each side (or vertex) three transcendental functions must be evaluated including the square-root function for R_n, the logarithmic function which occurs in the source potential, and the arctangent in the dipole potential. Moreover, there is some loss in accuracy of the algorithms based on (2.11) and (3.10) when the field point is very far away from the panel.

To overcome the latter problem, and provide a more efficient approach in terms of computing time, it is desirable to replace the exact expressions by multipole approximations when the field point is sufficiently far from the panel. This alternative is emphasized by Hess and Smith [1–3].

Appropriate far-field expansions for (2.1) and (3.1) can be derived from Taylor series involving products of partial derivatives of $1/r$ with appropriate moments of the panel area. Thus the source potential can be expanded in the form

$$\Psi = \iint r^{-1}\, \mathrm{d}\xi\, \mathrm{d}\eta$$

$$= \sum_{m=0}^{\infty} \sum_{n=0}^{\infty} \frac{(-)^{m+n}}{m!n!} I_{mn} \frac{\partial^{m+n}}{\partial x^m\, \partial y^n} \left(x^2 + y^2 + z^2\right)^{-1/2} \tag{6.1}$$

where

$$I_{mn} = \iint \xi^m \eta^n\, \mathrm{d}\xi\, \mathrm{d}\eta \tag{6.2}$$

is the corresponding moment of the panel about the origin. This series is convergent provided the field point is farther from the origin than any point on the panel. It can be truncated at a finite order $(m + n)$, provided the distance to the field point is sufficiently large to ensure the desired degree of accuracy.

The corresponding expansion for the dipole potential (2.1) is identical to (6.1) except for an additional derivative with respect to the coordinate z. The expansions for the higher-order distributions considered in Sections 4 and 5 are the same, except that the order of the moment I_{mn} is incremented by the corresponding integer powers of the distribution.

Note that only one evaluation of the square-root function is required in (6.1), to evaluate the (reciprocal) distance between the origin and the field point, since this is a

common factor in all of the derivatives. Thus the computational burden associated with transcendental functions is reduced from 12 to 1 per panel, when the multipole expansion is used in place of the closed-form results in Sections 2–5.

In the implementation described by Hess and Smith, (6.1) is truncated after the terms $m+n=2$, and the terms proportional to first moments are avoided by locating the origin at the centroid of the panel. Thus a total of four terms are included in (6.1), and in the corresponding approximation for the dipole potential. If this procedure is extended to include third- and fourth-order moments, a total of 13 terms are involved, but smaller values of the distance to the field point can be accommodated with the same degree of accuracy. Thus the fourth-order truncation provides an effective intermediate procedure to implement between the second-order multipole expansion and the exact formulae.

The moments (6.2) should be evaluated initially, for each panel, and stored for subsequent use with each appropriate field point. These pre-computed moments may be multiplied by the first factor in the double-series (6.1) to minimize the subsequent operations.

An algorithm for evaluating the moments (6.2) up to an arbitrary order can be developed starting with the y-integration:

$$I_{mn}=\iint \xi^m \eta^n \, d\xi \, d\eta = -\frac{1}{n+1}\oint \xi^m [\eta(\xi)]^{n+1} \, d\xi$$

$$=\frac{1}{n+1}\sum_{k=1}^{4}\int_{\xi_k}^{\xi_{k+1}} \xi^m [\eta(\xi)]^{n+1} \, d\xi. \tag{6.3}$$

The subsequent procedure is illustrated for the first term ($k=1$) over the side 1. Integrating by parts, the contribution to (6.3) is

$$I_{mn}^{(1)}=\frac{1}{(m+1)(n+1)}\int_{\xi_1}^{\xi_2} d\xi^{m+1}\eta^{n+1}$$

$$=\frac{1}{(m+1)(n+1)}\left(\xi_2^{m+1}\eta_2^{n+1}-\xi_1^{m+1}\eta_1^{n+1}\right)-\frac{\tan\theta_1}{m+1}\int_{\xi_1}^{\xi_2}\xi^{m+1}\eta^n \, d\xi$$

$$=\frac{1}{(m+1)(n+1)}\left(\xi_2^{m+1}\eta_2^{n+1}-\xi_1^{m+1}\eta_1^{n+1}\right)-\frac{n\tan\theta_1}{m+1}I_{m+1,n-1}^{(1)}. \tag{6.4}$$

The last result provides a recursion relation between the different moments of the same order, on the diagonal $m+n=$ constant. A starting value for $n=0$ is obtained by evaluating the last integral in (6.4),

$$I_{m0}^{(1)}=\frac{1}{m+1}\left(\xi_2^{m+1}\eta_2-\xi_1^{m+1}\eta_1\right)-\frac{\tan\theta_1}{(m+1)(m+2)}\left(\xi_2^{m+2}-\xi_1^{m+2}\right). \tag{6.5}$$

However, this scheme is ill-conditioned on a side where the tangent approaches infinity. As an alternative, we modify the recursion in (6.4) by solving for the moment in the last term, and after incrementing the indices it follows that

$$I_{mn}^{(1)}=\frac{\cot\theta_1}{(n+1)(n+2)}\left(\xi_2^m\eta_2^{n+2}-\xi_1^m\eta_1^{n+2}\right)-\frac{m\cot\theta_1}{n+1}I_{m-1,n+1}. \tag{6.6}$$

The starting value for $m = 0$ is obtained by deleting the last term in this equation. A general recursion scheme is then obtained by using (6.4–6.5) or (6.6), respectively, according as $|\tan \theta|$ is less than or greater than one.

7. Applications and extensions

The potentials which have been evaluated in the preceding sections are fundamental matrix elements of three-dimensional panel methods based either on an assumed source distribution, or on the solution of Green's theorem for the velocity potential.

From the standpoint of practical implementation, the efficient evaluation of these potentials is essential if the number of panels used to represent a body is large. A carefully-developed subroutine which evaluates the constant-strength potentials Ψ and Φ using (2.14) and (3.10) in single precision requires about 1.5 millisecond on a VAX 11/750. The alternative multipole approximation based on (6.1) and including moments of order two requires about 0.2 ms. on the VAX. The extended multipole approximation with moments up to order four requires about 0.4 ms, and therefore provides an effective algorithm for intermediate distances to the field point.

Possible extensions of this analysis include a more comprehensive treatment of curvilinear panels, and the development of efficient algorithms for integrating these potentials in the Galerkin sense over an arbitrary panel.

With respect to curvilinear panels, we have shown that the potential for a normal dipole distribution of constant moment can be readily derived, subject only to the restriction that the panel boundaries are straight segments. This result is independent of the precise panel shape. The corresponding results for the source distribution, and for higher-order distributions of both types, are expected to be more complicated, and to depend on the specific description of the panel surface.

The solution of boundary-integral equations by the Galerkin technique requires a second integration, over each panel of the body, with appropriate polynomial weight functions corresponding to the distributions of the singularities themselves. It appears that this second integration must be performed numerically, and special attention is required when the second panel is identical or adjacent to the first.

Acknowledgements

This work was sponsored by the National Science Foundation (Grant 8210649-A01-MEA), and by the Office of Naval Research (Contract N0014-82-K-0198).

References

[1] Hess, J.L. and Smith, A.M.O., *Calculation of non-lifting potential flow about arbitrary three-dimensional bodies*, Report No. E.S. 40622, Douglas Aircraft Company, Inc., Long Beach, CA (1962).

[2] Hess, J.L. and Smith, A.M.O., Calculation of non-lifting potential flow about arbitrary three-dimensional bodies, *J. Ship Res.* 8, 2 (1964) 22–44.

[3] Hess, J.L. and Smith, A.M.O., Calculation of potential flow about arbitrary bodies, *Progress in Aero. Sci.* 8 (1966) 1–138.

[4] Yeung, R.W., *A singularity-distribution method for free-surface flow problems with an oscillating body*, Report No. NA 73-6, College of Eng'g., Univ. of Cal., Berkeley (1973). (See also Bai, K.J., and Yeung, R.W., Numerical solutions to free-surface flow problems, *Proc. 10th Symp. Naval Hydro.* (1974) 631–633).

[5] Webster, W.C., The flow about arbitrary three-dimensional smooth bodies, *J. Ship Res.* 19, 4 (1975) 206–218.